Netshape centrifugal gel-casting of high-temperature sialon ceramics

Jamshidi, Parastoo; Lu, Nannan; Liu, Gang; Herny, Emilie ; Attallah, Moataz

DOI:
10.1016/j.ceramint.2017.11.143
10.1016/j.ceramint.2017.11.143

Document Version
Peer reviewed version

Citation for published version (Harvard):
Jamshidi, N, Lu, N, Liu, G, Herny, E & Attallah, M 2017, 'Netshape centrifugal gel-casting of high-temperature sialon ceramics', Ceramics International. https://doi.org/10.1016/j.ceramint.2017.11.143, https://doi.org/10.1016/j.ceramint.2017.11.143

Netshape Centrifugal Gel-casting of High-Temperature Sialon Ceramics

Parastoo Jamshidi[1], Nannan Lu[1], Gang Liu[2], Emilie Herny[3], and Moataz M. Attallah[1]

[1] School of Metallurgy and Materials, University of Birmingham, Edgbaston, B15 2TT, UK

[2]Faculty of Materials and Energy, Southwest University, 400715 Chongqing, China

[3]Microturbo, 31019 Toulouse Cedex 2, France

Abstract

Gel-casting of ceramics is a promising technique that can be used to manufacture complex structures in a netshape approach, with the density and mechanical properties of the green and sintered structures being strongly influenced by the composition of the gel formulation and the casting approach. In this study, a parametric study was performed to assess the influence of the gel formulation (solid loading and resin content), the casting approach (centrifugal casting versus gravity casting), and the sintering treatment on the microstructural and mechanical properties development in gel-cast sialon ceramics. Optimum levels of solid loading and resin content were identified for the gel formulation. The study showed that a significant improvement in the high temperature flexural strength (~1.5-2 folds) can be achieved by employing a centrifugal gel-casting approach, due to the reduction of the porosity caused by the entrapped gas that gets entrapped during the standard casting process.

Key words: Gel-casting; Sialon Ceramics; Mechanical Properties

1. Introduction

High performance advanced ceramics have continuously gained an increasing interest in various industrial applications due to their distinct properties of low density, very high compressive strength, good thermal shock resistance, and their exceptional resistance to wetting or corrosion, operating cost effectively in today's market demand [1, 2]. One of the strongest and most durable ceramic materials is Sialons, the advanced silicon nitride based ceramics, which is the world's first commercially available advanced ceramic alloy [3].

In the case of SiAlONs, Si is substituted by Al in silicon nitride, with a corresponding atomic replacement of N by O, to satisfy valency requirements. The resulting 'solution' (sialon) has superior properties to the original pure solvent (silicon nitride) [4].

An ideal technique for the fabrication of simple or complex dense ceramic components with a wide range of shapes and sizes would be a process that possesses a capability to produce components with i) very homogeneous material properties, ii) high green strength and density, iii) excellent green body machinability, iv) a requirement for small quantities of organic binder, which does not include the critical binder removal step, and v) low capital equipment cost. Various colloidal forming processes have been investigated in the literature. These techniques result in a homogenous green microstructure with reduced production costs for advanced ceramics. One of these techniques is gel-casting (GC) [5, 6], which is a near netshape forming technique that has been used for making high-quality complex ceramic parts via an in-situ polymerisation process that immobilises the ceramic particles allowing them to hold the shape of the mould [7].

This technique has superior advantages over other ceramics forming processes such as injection moulding, which has limited applications due to its long binder removal time, and slip casting, due to its slow casting rate and poor green strength that makes the castings too

fragile for machining. GC offers several advantages, including short process time, high yields, high green capacity, low organic content that translates into easy binder removal, reasonable machinability of the green body, and low capital equipment cost [8].

The overall success of the process depends on several important factors including; a) the optimisation of the slurry formulation, as it is essential to use highly loaded ceramic slurries with a reasonably low viscosity to reduce the drying shrinkage, and thus minimise the build-up of stresses during drying and sintering, b) performing a sufficient de-airing step prior to casting to avoid any defects that can form due to the entrapment of air bubbles during casting, and c) using a mould with the appropriate material properties to create a flexible mould that can allow shrinkage to occur with a reduced build-up of stresses in the cast part during drying [9]. Despite these attributes, very few studies [10] investigated the optimisation of the gel formulation and the casting approach to manufacture complex structures in a netshape approach, while achieving the appropriate microstructure and mechanical properties after sintering.

To produce high strength Sialons GC components, vacuum de-airing is required, especially when using a high solid loading. However, vacuum de-airing is often insufficient to entirely remove all the residual air bubbles, resulting in entrapped bubbles within the green component, which remain in the component after sintering. As such, the use of centrifugation during casting can overcome this issue compared with vacuum de-airing, since the residual bubbles will be forced out of the gel under the action of the centrifugal force. There are several studies that verified the utility of centrifugation on the elimination of the residual air bubbles within the slurry, resulting in an increase in strength following sintering [11]. The addition of centrifugation to the conventional GC route was shown previously to have been greatly effective in eliminating the entrapped air in concentrated ceramics slurries, alongside an enhanced consolidation and densification in the green component [11-13].

There has not yet been, however, any study to investigate the utility of centrifugation during GC as a means to improve the density and the microstructural homogeneity in GC sialon ceramics. In this study, a parametric study was performed to assess the influence of the formulation composition (solid loading and resin content), the casting approach (centrifugal-assisted GC versus gravity GC), and the sintering treatment on the microstructural and mechanical properties development in gel-cast sialons ceramics. A large matrix of conditions has been investigated to optimise the conventional GC route, where the solid loading and the resin content were varied. In addition to de-airing in a vacuum system step after casting, a centrifuging step was added into the route, which is in itself a further de-airing step through the action of the centrifugal force on the entrapped bubbles.

Various rotational (centrifugation) speeds were used to obtain an optimum condition with the lowest level of porosity and significantly increased level of high temperature strength compared to un-centrifuged conventional GC. The green density, sintered density, structural integrity, microstructure, and porosity of the samples were measured and characterised to find the optimum parameters required to produce dense and homogeneous components using this approach.

2. Experimental Methods

2.1. Materials and slurry preparation

The Syalon 050 powder used in this study was produced using spray drying, and supplied by International Syalons (Newcastle), England, UK. The powder morphology, size, and sintering behaviour were characterised using a JEOL700 field emission gun scanning electron microscope (FEG-SEM) operated at 10-20 kV, a SYMPATEC HELOS particle size analyser (BET, ASAP 2010, Micromeritics), and a Netzsch dilatometer, respectively. Differential scanning calorimetry (DSC) (Perkin Elmer DSC7, UK) was employed to detect the

decomposition temperature of the polymers within the green body. DSC/TGA was conducted in air under a heating rate of 10 ˚C/min, using a ~15 mg sample.

To prepare the green body samples, ethylene glycol diglycidyl ether (EGDE, Nasage, Japan) was used as an epoxy resin, alongside ammonium polyacrylate (NH_4PAA) dispersant (Allied Colloids, Bradford, UK), and bis(3-aminopro-pyl)amine (Sigma-Aldrich, Germany) as a hardener, for slurry preparation, following the approach developed in our previous study [10], and other reports in the literature [14].

An aqueous solution containing EGDE epoxy resin was prepared by dissolving it in a mixture of distilled water and NH_4PAA dispersant, prior to slurry preparation. The commercial syalon 050 powder (surface area 11.96 cm^2/g) was slowly added into the pre-mixed solution under constant stirring, with various solid-loading levels in a parametric study. The slurries were ball milled overnight with alumina milling media. The hardener was added into the slurries and mixed prior to casting. The resulting slurries were then cast into plastic moulds of the desired shape, then degassed in a vacuum system to aid the moulding process and for further de-airing to prevent air entrapment. After drying at room temperature for 24 hours, demoulding was carefully performed, followed by transferring the green bodies into a 40˚C oven for further drying for 24 hours prior to sintering. The green bodies were subsequently sintered to investigate the effect of the sintering treatment on the porosity level, microstructural development, and mechanical properties. A burnout procedure was initially performed, followed by sintering at 1730 ˚C in nitrogen for 4 hours.

To find the optimum process parameters required to produce dense and homogeneous components, GC samples with different resin and solid loading contents were made with and without a centrifugation step (Table 1).

To investigate the effect of centrifugation on the homogeneity of samples, cylindrical samples of Ø 25 × 50 mm with 44.5 vol. % solid loading, 25 wt. % resin content, and 2500 rotation per minute (rpm) centrifugal speed were prepared under same conventional GC route including de-gassing in a vacuum system completed with addition of centrifugation step. They were cut into five small cylinder samples (Ø25×10 mm), the density of every disc was measured using the Archimedes density measurement method.

2.2. Characterisation of GC Sialons samples with various parameters

2.2.1. Density measurement

The densities of the green bodies and the sintered samples prepared with different solid loading, resin content and various centrifuge rotational speeds were measured using the Archimedes principle. All the samples were put into distilled water for 24 hours to fill the surface air bubbles with water. The samples weight in air (dry weight) and water (wet weight, room temperature) were measured. The density of the samples was calculated based on Archimedes' principle equation (1) as follows (ASTM, 2015):

$$\rho = \frac{M_{dry} \cdot \rho_{water}}{M_{dry} - M_{wet}} \qquad \text{Eq. 1}$$

where ρ is sample density, M_{dry} is sample weight in air, M_{wet} is sample weight in water, and ρ_{water} is the density of water at room temperature, 1 g/cm^3.

2.2.2. Optical Microscopy and Scanning Electron Microscopy

Optical microscopy was carried out using a Zeiss optical microscope, fitted with a digital camera and an automated stage to characterise the porosity distribution across the samples. Examination of large areas was achieved through automated image capture and multiple

image stitching. The porosity area fraction was calculated using ImageJ software, and subsequently translated into volume fraction using:

$$d_v = {d_s}^{3/2} \qquad \text{Eq. 2}$$

Where d_v is volume fraction, and d_s is the pore surface (area) fraction.

To analyse the microstructure and defect level within the fabricated samples with different solid loading, resin content, and various centrifuge rotational speeds, a Quanta200 SEM, equipped with energy dispersive EDX (INCA x-sight, oxford analytical instrument, UK) was utilised.

2.2.3. Micro-computer tomography

GC samples fabricated using the optimised process parameters, with and without centrifuging, were also scanned using a Skyscan1172 micro-computer tomography (micro-CT) system (Bruker, Belgium), with 80 kV maximum X-ray energy, 8 W beam power, 570 ms exposure per projection, aluminium filter, and 6.76 μm pixel size. Qualitative and quantitative analyses were performed on the data to assess the integrity of the internal structure and the volume fraction of porosity within the fabricated matrix. The scanned data were reconstructed into a 3-dimensional volume using NRecon Software, producing images with a resolution of ~5 μm. Following reconstruction, images analysis and thresholding were performed by CTan software. 3D visualisations were constructed for the total volume of interest using CTVox software.

2.2.4. Four-point flexural strength testing

The influence of centrifugation on controlling the level of porosity of the GC samples following sintering was assessed using four-point flexural strength test under different test

temperatures (room temperature, 700˚C, and 900˚C) using the procedure given in EN843-5. The size of the sintered test bars was 4.5 mm × 3 mm × 50 mm length. The tests were performed at the National Physical Laboratory (NPL), UK.

3. Result and Discussion

The morphology of the sialon powder used in this study is shown in figure 1a. SEM micrographs of the powders showed near spherical particles, or doughnut-shaped particles with internal pores containing small irregularly-shaped particles inside. The particle size was between 7 μm to 100 μm, with d_{50} of 44.9 μm (using data obtained from the particle size analyser, not shown here). Figure 1b shows the dilatometry trace for the sialon powder, which was cycled to 1450˚C. The powder was pressed into a cylindrical bar of dimensions Ø 5 × 15 mm for the test. Initially, the sample experienced expansion to ~1200˚C, beyond which the sample started to densify. It is clear that densification occurs at the same temperature as the formation of the oxide liquid phase at about 1200-1250˚C [15, 16]. The composite starts to densify in this temperature range mainly because of the rearrangement of the Si_3N_4 particles [17].

In order to identify the temperature range for the binder burnout process, DSC-TG was performed on the green GC sample to study the thermal behaviour. Figure 2 shows the DSC-TG curve of a green sample, which was cast using 44.5 vol.% slurry with 25 wt.% resin content in the premixed solution. The thermal decomposition of the polymer started at ~200˚C and finished at ~600˚C. Therefore, the binder burnout temperature for the GC samples was chosen to be 600˚C. The burnout process was followed by sintering at 1730˚C in nitrogen for 4 hours.

An extensive matrix of conditions was investigated to optimise the GC route, where the solid loading and the resin content were varied, with and without centrifugation. The influence of

centrifugation rotation speeds on the density, porosity and homogeneity of the samples were studied. The density of the green bodies and sintered samples prepared with various process parameters was measured using Archimedes principle (Table 2). Based on our previous rheological study [10], a solid loading of 44.5 vol. % was selected as the highest possible solid loading, yielding a sufficiently low viscosity with a reasonable fluidity for slurry preparation. Using this solid loading, homogeneous and crack free sintered castings can be obtained.

It was found out that the density variation between the samples with different resin contents was insignificant. Samples prepared with centrifugal gel casting (CGC), however are significantly denser (samples 1-5) than the samples created by conventional GC (samples 6-8) ($p<0.05$) (Table 2). The density only slightly increased by increasing the rotation speed. This is attributed to the increasing formation of compacted powders sedimentation in the colloidal system with the increase in the centrifugal force. The effect of this unique compaction mechanism of centrifugal compaction has been previously reported in the literature [11, 13]. In such a process, the particles flow downwards, in the opposite direction of the medium in the colloidal system, to form densely packed and compacted sediment, resulting in a highly dense part. Table 2 also shows the density changes after sintering. After sintering, the density of the CGC samples were significantly higher, nearly 100% of the theoretical density, highlighting the role of using an optimum sintering treatment to enhance the consolidation of the GC parts [18]. The influence of the resin content of the sialon slurry and centrifuge rotation speed on the green density of the GC and CGC samples is shown in figure 3. The highest green density was obtained when the sample with a resin content of 20 wt. % was centrifuged at 6000 rpm. After sintering, the CGC samples containing 20 wt. % resin and solid loading of 44.5 vol. % were fully dense (Table 2).

The effect of centrifugation rotation speed on the elimination of defects (air bubble and voids) within the sample with solid loading of 44.5 vol. % and resin content of 20 wt. % (as optimum parameters) was investigated. CGC (6000 rpm) and conventional GC samples were sectioned and examined under the microscope. Figure 4a shows the significant differences in surface pore content of the two samples made by GC and CGC. It is obvious that the surface of the conventional GC sample contains many pores (entrapped air), while the CGC sample is effectively pore-free.

Examination of the samples using optical microscopy showed that in the case of the conventional GC sample (Figure 4b), spherical pores with diameters from 1 to 500 μm were present throughout the structure, whereas the CGC sample (Figure 4c) showed significantly finer pores that were present mostly along the axial direction, as well as along the direction of the centrifugal force. It can be observed that at the bottom section, the porosity is lower than at the top. These observations confirm that centrifugation lowered the level of porosity within the sample matrix. In fact, it can be rather difficult to remove the entrapped air in the ceramic slurry with the high solid loading by vacuum de-airing due to its high viscosity [11]. The addition of centrifugation to the conventional GC route was shown previously to have been greatly effective in eliminating entrapped air in concentrated ceramics slurries [12].

The influence of the rotation speed on the porosity content was investigated. Samples with solid loading of 44.5 vol. %, resin content of 20 wt. % (the optimum slurry composition) and centrifuge rotational speeds of 4000, 6000, and 8000 rpm were cast. The samples were sectioned and the porosity content was investigated quantitatively (Figure 5a) and qualitatively (Figure 6), within the top, middle and bottom sections of the samples. A conventional GC sample with the same solid loading and resin content was used as a control

sample. It was found that the control sample contained high porosity levels (Figure 5a). However, the CGC samples showed lower porosity levels. The effect of the rotation speed on the porosity variation within the samples was investigated within three different sections of the samples. The minimum level of porosity was found at the bottom, and increasing towards the top of all three CGC samples. The lowest average porosity was obtained using a rotation speed of 6000 rpm.

The influence of the resin content at a constant rotation speed on the volume fraction of porosity within the matrix was also investigated (Figure 5b). It was further confirmed that the sample with 20 wt. % resin content showed the lowest level of porosity throughout the sample, compared with the other tested CGC sample conditions. The significant effect of centrifugation is clearly shown in Figure 5b. The levels of porosity within the samples were significantly improved in the CGG samples. Among the CGC samples, the highest porosity was present in the conditions with a resin content of 25-30 wt. %. This is attributed to the low green density in these samples with the high resin content, alongside the significant weight loss and shrinkage, leading to high porosity [19]. The volume fraction, size, and velocity of the entrapped air bubbles in ceramic slurries are known to be dependent on a number of variables, including the solid loading, viscosity of the slurry, and densities of the liquid and particles in the ceramic slurry. The entrapped bubbles are categorised into two classes; inter-agglomerate (also called free bubbles) and intra-agglomerate air bubbles. The former is commonly generated either during slurry preparation due to the turbulent flow (e.g. during milling or stirring), or because of the eruption of a large amount of entrapped air inside highly agglomerated powders within the slurry. They move freely within the slurry among the particles. Conversely, the intra-agglomerates bubbles are attached to the particles, and their movement is restricted by the surrounding particles. Bubbles of the latter type are formed when the entrapped air cannot be released from the agglomerates. The velocity and

moving direction (e.g. sink or rise) of the intra-agglomerate bubbles are dependent on the bubble density and their coordination number [12, 20, 21]. In the case of sample 3 (20 wt.% resin-8000 rpm), it is likely that the high level of porosity within the top section is attributed to intra-agglomerates bubbles. In fact, high centrifugal speeds have previously been reported to cause inhomogeneity, pore propagation, and Y-shaped crack formation [13].

To further examine the effect of centrifugation on the porosity distribution within the CGC samples, SEM images of the microstructure were taken at five different sections across the sample with the optimum parameters (sample 2), ranging from the top to the bottom of the sample (Figure 6). Pores were found in the axial direction, as well as in the direction of the centrifugal force, tending to decrease from top to bottom (Figure 6 (5-1)), indicating the collection of the escaped air bubbles to the top section due to the centrifugal force.

At the micro-level, the air bubbles in the slurry are subjected to two main forces during CGC; a relative centrifugal force (RCF) and a viscous drag force. In the centrifugation process, the sample was rotated in the horizontal plane. Therefore, particles in the slurry have the same rotational speed, but different rotational radii (and accordingly different forces). Because the particles at the bottom of the samples receive a higher centrifugal force, where it is easier to overcome the viscous drag force, particles at the bottom tend to move to the bottom. In contrast the air bubbles at the bottom are easier to be removed.

The integrity and internal structure of the CGC samples with the optimum condition (6000 rpm, 44.5vol%, and 20wt% resin) following sintering were analysed using micro-CT. Figure 7a shows a 3D-CT volume model and the outer structure of the fabricated sample. No obvious pores or cracks were observed. The level of porosity along the GC and CGC samples is shown in Figure 7b. It can be seen that more internal pores and voids are present within

matrix of the convectional GC sample. Uniform samples with virtually no porosity were obtained using CGC (Figure 7b).

To evaluate the effect of centrifuging on the mechanical properties of CGC and GC samples, 4-point flexural strength tests were conducted under different temperatures following high temperature sintering. Cylindrical CGC samples (figure 8a) were prepared using the optimised processing conditions of (44.5 vol. % - 20 wt. % - 6000 rpm) for mechanical testing. The castings were cut into long bars then sintered, as shown in Figure 8b.

As Figure 8c shows the flexural strength increased significantly ($p<0.001$) in the sintered CGC samples when the optimised process conditions were used, whereas the conventional (un-centrifuged) GC samples exhibited poorer mechanical properties due to their relatively lower density and the presence of porosity within the sample matrix. The flexural strength of CGC samples increased by ~1.5 folds in the CGC samples (from 295.2 ± 38 in conventional GC to 450.6 ±52.4 MPa at room temperature in the optimised CGC). This confirms the great impact of centrifuging on the elimination of air bubbles and the subsequent full consolidation of the compact density due to sintering.

The flexural strength of CGC samples at high temperature of 700 ˚C and 900 ˚C was also shown a significant increase ($p<0.05$). This suggests that the CGC samples can retain their strength even at higher temperatures. The flexural strength nearly doubled when the density of the GC samples was improved by adding the centrifugation step into the GC route.

To evaluate the impact of CGC after high temperature sintering on the geometrical shrinkage, the diameter and height of the samples were measured before and after sintering. The

shrinkage was measured on disc shape samples in the radial and axial directions (D1 and D2), as shown in Table 4. The average shrinkage in the radial and axial directions was 18.4% and 27.4%, respectively. Less shrinkage in the radial direction was obtained in the sintered CGC samples (~25%) compared with extent of shrinkage in the same direction for sintered GC samples without centrifuging, which suggests that denser CGC samples results in less shrinkage.

4. Conclusions

In this study, optimised processing conditions were developed for netshape CGC of high-temperature sialons ceramics. A slurry of 44.5 vol% solid loading, 20 % resin content, alongside a centrifugation step at a rotational speed of 6000 rpm were found to be optimal to produce fully dense samples after sintering, with virtually no porosity throughout the samples when compared to conventional GC. It was shown that the addition of centrifugation into the conventional route effectively densified the GC samples, as well as reduced the level of porosity within the sample matrix, in both the green and sintered conditions. The mechanical properties of CGC samples significantly increased compared with the conventional GC samples. Also, the high temperature mechanical properties increased, indicating that CGC can retain their mechanical properties at elevated temperatures. Furthermore, the extent of shrinkage decreased significantly in the CGC samples, compared with conventional GC. This highlights the significant potential of this route in netshape processing of complex ceramic shapes.

Acknowledgements

The authors would like to acknowledge the financial support from MicroTurbo/Safran Group. The support of the Innovation and Technology Partnership (ITP) is highly appreciated.

References

1. Schmidt, S., S. Beyer, H. Knabe, R. Immich, A. Meistring, and A. Gessler. *Advanced ceramic matrix composite materials for current and future propulsion technology applications.* Acta Astronautica, 2004. **55**(3–9): p. 409-420.
2. Bansal, N.P., *Handbook of ceramic composites*. Vol. 200. 2006: Springer Science & Business Media.
3. Cao, G. and R. Metselaar, . *alpha.'-Sialon ceramics: a review.* Chemistry of Materials, 1991. **3**(2): p. 242-252.
4. Ekström, T. and M. Nygren, *SiAlON ceramics.* Journal of the American Ceramic Society, 1992. **75**(2): p. 259-276.
5. Omatete, O.O., M.A. Janney, and S.D. Nunn, *Gelcasting: From laboratory development toward industrial production.* Journal of the European Ceramic Society, 1997. **17**(2–3): p. 407-413.
6. Yang, J., J. Yu, and Y. Huang, *Recent developments in gelcasting of ceramics.* Journal of the European Ceramic Society, 2011. **31**(14): p. 2569-2591.
7. Gilissen, R., et al., *Gelcasting, a near net shape technique.* Materials & Design, 2000. **21**(4): p. 251-257.
8. Vandeperre, L., A. De Wilde, and J. Luyten, *Gelatin gelcasting of ceramic components.* Journal of Materials Processing Technology, 2003. **135**(2): p. 312-316.
9. Dhara, S., et al., *Shape forming of ceramics via gelcasting of aqueous particulate slurries.* Bulletin of Materials Science, 2002. **25**(6): p. 565-568.
10. Liu, G., et al., *Gel casting of sialon ceramics based on water soluble epoxy resin.* Ceramics International, 2015. **41**(9, Part A): p. 11534-11538.
11. Maleksaeedi, S., M.H. Paydar, and J. Ma, *Centrifugal gel casting: a combined process for the consolidation of homogenous and reliable ceramics.* Journal of the American Ceramic Society, 2010. **93**(2): p. 413-419.
12. Maleksaeedi, S., M.H. Paydar, and J. Ma, *Centrifugal deairing of concentrated ceramic slurries.* Journal of the American Ceramic Society, 2009. **92**(12): p. 2861-2869.
13. Suzuki, H.Y., *Dense and Homogeneous Compaction of Fine Ceramic and Metallic Powders: High-Speed Centrifugal Compaction Process.* AIP Conference Proceedings, 2008. **973**(1): p. 586-591.
14. Mao, X.J., Shimai, S., Dong, M., Wang, S., *Gelcasting of Alumina using Epoxy Resin as a Gelling Agent*. Journal of the American Ceramic Society, 2007, 90(3):986-988;
15. Mallik, A.K., et al., *A comparative study of SiAlON ceramics.* Ceramics International, 2012. **38**(7): p. 5757-5767.
16. Herrmann, M., S. Höhn, and A. Bales, *Kinetics of rare earth incorporation and its role in densification and microstructure formation of α-Sialon.* Journal of the European Ceramic Society, 2012. **32**(7): p. 1313-1319.
17. Garrett, J.C., et al., *cBN reinforced Y-α-SiAlON composites.* Journal of the European Ceramic Society, 2013. **33**(11): p. 2191-2198.
18. Koch, D., et al., *Evolution of porosity by freeze casting and sintering of sol-gel derived ceramics.* Journal of sol-gel science and technology, 2003. **26**(1-3): p. 149-152.
19. Zhang, W., H. Wang, and Z. Jin, *Gel casting and properties of porous silicon carbide/silicon nitride composite ceramics.* Materials Letters, 2005. **59**(2): p. 250-256.
20. Bhaga, D. and M. Weber, *Bubbles in viscous liquids: shapes, wakes and velocities.* Journal of Fluid Mechanics, 1981. **105**: p. 61-85.

21. Dewsbury, K., D. Karamanev, and A. Margaritis, *Hydrodynamic characteristics of free rise of light solid particles and gas bubbles in non-Newtonian liquids.* Chemical engineering science, 1999. **54**(21): p. 4825-4830.

Figure captions:

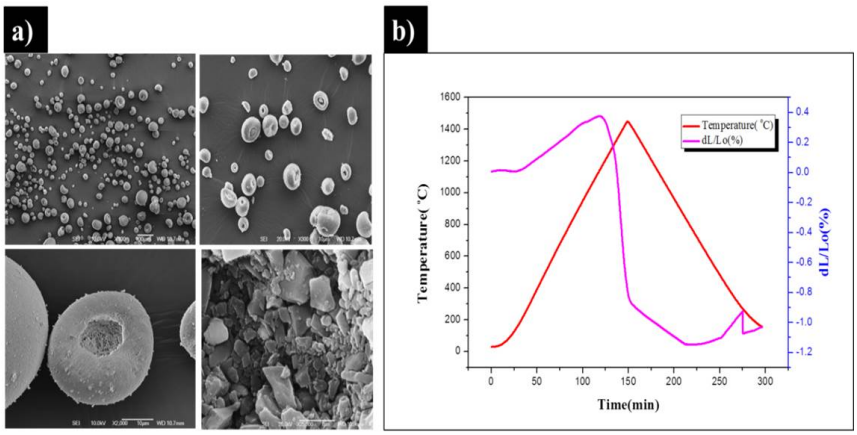

Figure 1: a) SEM micrograph showing the morphology and the size distribution of Sialon powders prepared by spray drying method at different magnifications, b) dilatometry results of the as-received sialon 050 powder.

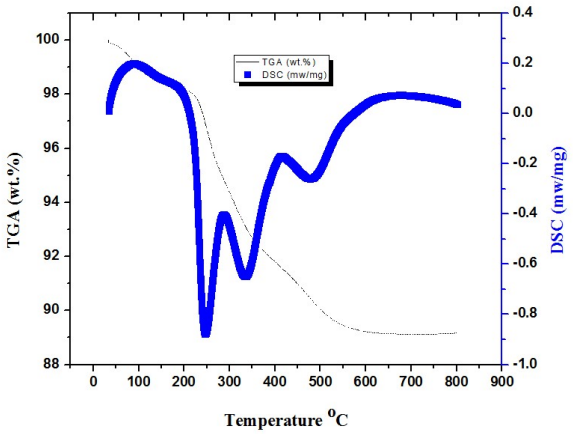

Figure 2: DSC-TGA thermal analysis of the green sample obtained from 44.5 vol.% slurry with 25 wt.% resin content.

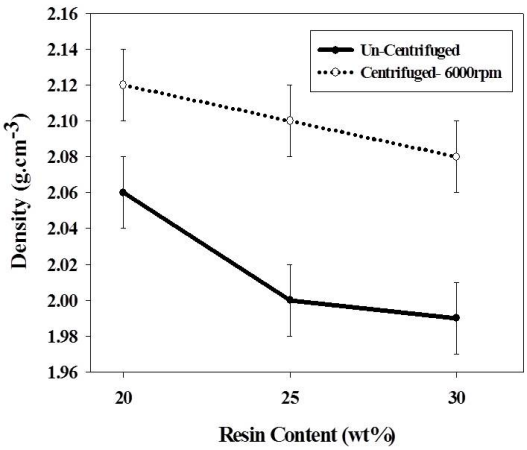

Figure 3: The density of the Sialons green body samples prepared with different resin contents (using centrifugation at 6000 rpm) and without centrifugation.

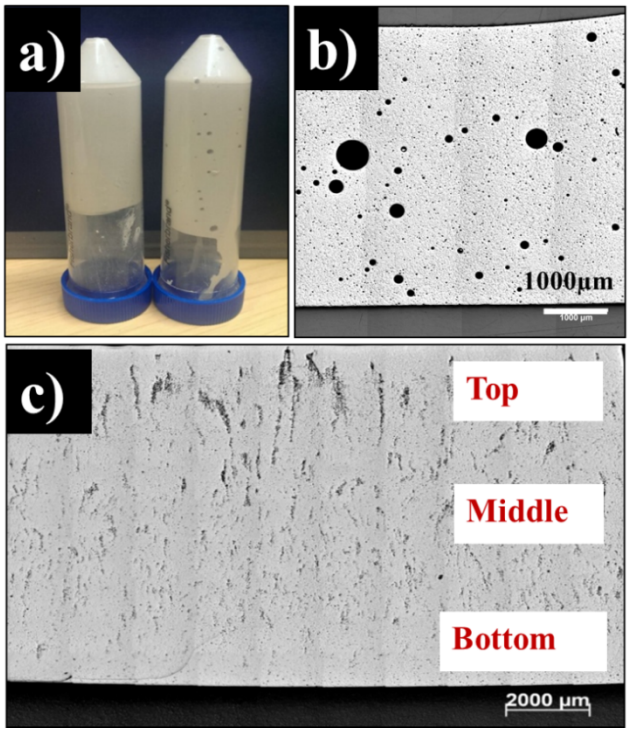

Figure 4: Images and micrographs for the GC and CGC samples, a) illustrating the role of centrifuging on porosity (centrifuged sample with fewer pores (left) and un-centrifuged samples with surface connected pores (right), b) optical micrographs from one section of conventional GC samples and c) CGC sialons samples.

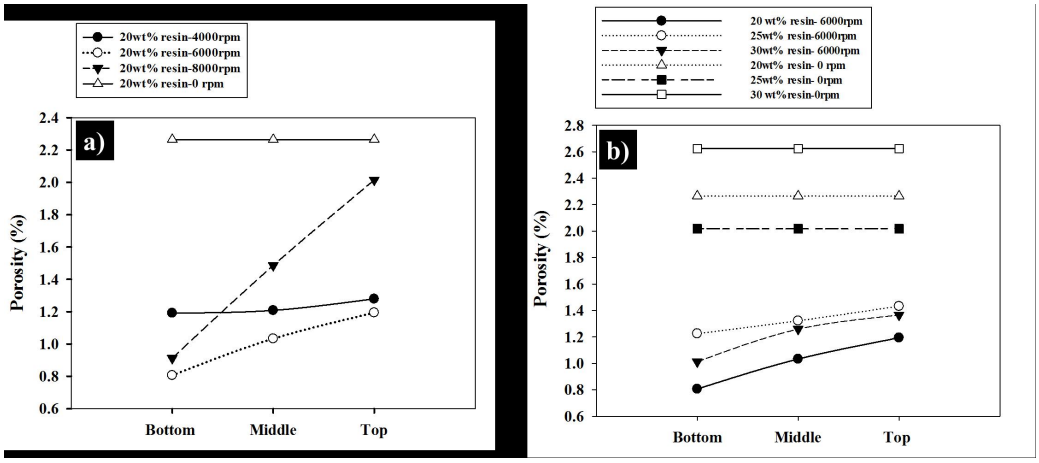

Figure 5: Porosity variation within the CGC samples (form bottom to top), compared with conventional GC (control) samples, showing: a) samples prepared with the same resin content and various centrifugal rotational speeds, and b) samples prepared with the same centrifugal speed and various resin contents.

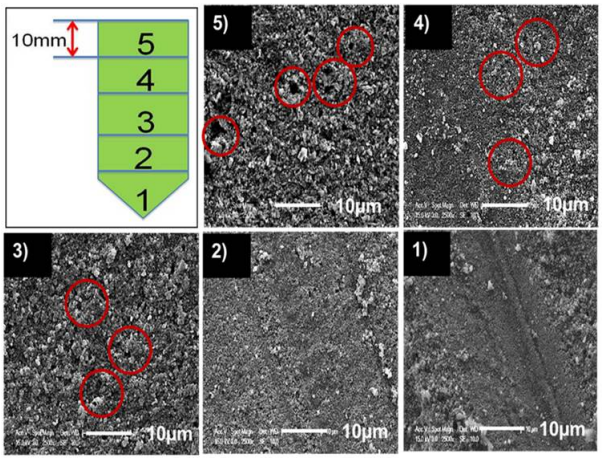

Figure 6: Schematic diagram of the samples prepared using CGC and SEM micrographs of 5 different sections from top to bottom. The circles show the presence of porosity within the samples in different sections.

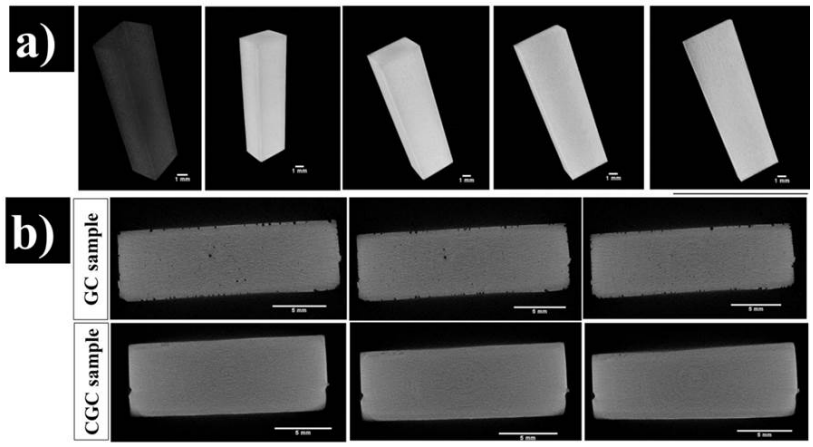

Figure 7: Representative results of a) 3D-CT volume model of sintered CGC sample illustrating a crack-free structure, with virtually no porosity, and b) cross-sectional micro CT grey scale slice at various sections of the samples of GC samples (top) and CGC samples (bottom).

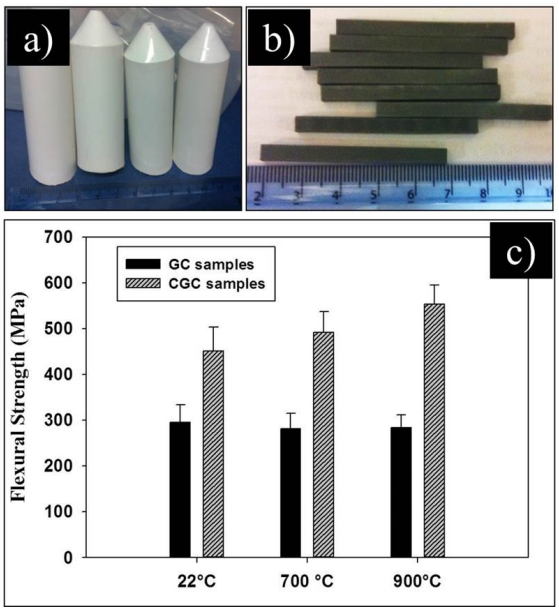

Figure 8: The mechanical properties of crack free and homogenous CGC samples: a) green body before sintering, b) sintered bars for mechanical testing, and c) four-point flexural strength results for GC and CGC samples . Results are displayed as an average of n=10 specimens ± standard deviation.

Table 1. Preparation of gel-cast samples with various process parameters

Sample	Parameters		
	Solid loading (vol%)	Resin content (wt%)	Centrifugal speed (rpm)
1	44.5	20	4000
2	44.5	20	6000
3	44.5	20	8000
4	44.5	25	6000
5	44.5	30	6000
6	44.5	20	0
7	44.5	25	0
8	44.5	30	0

Effect of rpm

Effect of resin content

Non- Centrifuged

Table 2. Density of green body and sintered gel-cast samples prepared with various parameters and centrifuging speed rate.

Green body		Sintered samples	
Sample	**Density ($g/cm^3 \pm 0.02$)**	**Absolute density (g/cm^3)**	**Density (%) Theoretical density**
1	**2.02**	**3.24**	**100.0**
2	**2.12**	**3.24**	**100.0**
3	**2.11**	**3.25**	**100.0**
4	**2.10**	**3.24**	**100.0**
5	**2.08**	**3.25**	**100.0**
6	**2.06**	**3.2**	**99.1**
7	**2.00**	**3.22**	**99.7**
8	**1.99**	**3.21**	**99.4**

Table 3. The geometry and shrinkage data for GC and CGC samples.

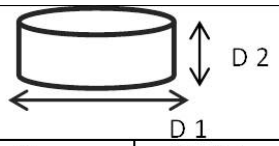

Sample	Green Ø/mm	Sinter Ø/mm	Shrinkage %	Mean Shrinkage %
D1-1	23.95	19.54	18.41	18.42
D1-2	23.97	19.55	18.43	
D2-1	12.15	8.65	28.81	27.36
D2-2	12.70	9.41	25.91	